Probe Molecule Chemisorption−Low Energy Ion Scattering Study of Surface Active Sites Present in the Orthorhombic Mo−V−(Te−Nb)−O Catalysts for Propane (Amm)oxidation

Vadim V. Guliants,* Rishabh Bhandari, Andrew R. Hughett, Salil Bhatt, and Benjamin D. Schuler

Department of Chemical and Material Engineering, University of Cincinnati, Cincinnati, Ohio 45221-0012

Hidde H. Brongersma and Arie Knoester

Calipso B.V. and Department of Applied Physics, Eindhoven University of Technology, P.O. Box 513, 5600 MB Eindhoven, The Netherlands

Anne M. Gaffney† and Scott Han

Rohm and Haas Co., 727 Norristown Road, Spring House, Pennsylvania 19477-0904

Received: November 20, 2005; In Final Form: February 7, 2006

Methanol and allyl alcohol chemisorption and surface reaction in combination with low energy ion scattering (LEIS) were employed to determine the outermost surface compositions and chemical nature of active surface sites present on the orthorhombic (M1) Mo−V−O and Mo−V−Te−Nb−O phases. These orthorhombic phases exhibited vastly different behavior in propane (amm)oxidation reactions and, therefore, represented highly promising model systems for the study of the surface active sites. The LEIS data for the Mo−V−Te−Nb−O catalyst indicated surface depletion for V (−23%) and Mo (−27%), and enrichments for Nb (+55%) and Te (+165%) with respect to its bulk composition. Only minor changes in the topmost surface composition were observed for this catalyst under the conditions of the LEIS experiments at 400 °C, which is a typical temperature employed in these propane transformation reactions. These findings strongly suggested that the bulk orthorhombic Mo−V−Te−Nb−O structure may function as a support for the unique active and selective surface monolayer in propane (amm)oxidation. Moreover, direct evidence was obtained that the topmost surface VO_x sites in the orthorhombic Mo−V−Te−Nb−O catalyst were preferentially covered by chemisorbed allyloxy species, whereas methanol was a significantly less discriminating probe molecule. The surface TeO_x and NbO_x sites on the Mo−V−Te−Nb−O catalyst were unable to chemisorb these probe molecules to the same extent as the VO_x and MoO_x sites. Our findings suggested that different surface locations for V^{5+} ions in the orthorhombic Mo−V−O and Mo−V−Te−Nb−O catalysts may be primarily responsible for vastly different catalytic behavior exhibited by the Mo−V−O and Mo−V−Te−Nb−O phases. Although the proposed isolated V^{5+} pentagonal bipyramidal sites in the orthorhombic Mo−V−O phase may be capable of converting propane to propylene with modest selectivity, the selective 8-electron transformation of propane to acrylic acid and acrylonitrile may require the presence of several surface VO_x redox sites lining the entrances to the hexagonal and heptagonal channels of the orthorhombic Mo−V−Te−Nb−O phase. The study of allyl alcohol oxidation over the Mo−V−O and Mo−V−Te−Nb−O catalysts further suggested that water plays a critical role during the oxidation of acrolein intermediate to acrylic acid over the orthorhombic (M1 phase) Mo−V−Te−Nb−O catalysts. Finally, the present study strongly indicated that chemical probe chemisorption combined with low energy ion scattering (LEIS) is a novel and highly promising surface characterization technique for the investigation of the active surface sites present in the bulk mixed metal oxides.

Introduction

The current abundance and low environmental impact of propane as a feedstock have generated considerable interest in oxidative catalytic conversion of propane to acrylic acid and acrylonitrile.[1−17] Recently discovered multicomponent Mo−V−Te(Sb)−Nb−O catalysts have shown great promise in propane oxidation to acrylic acid and ammoxidation to acrylonitrile.[4−11,18−24] These mixed-phase catalysts contain so-called "M1" and "M2" phases with orthorhombic and pseudohexagonal structures, respectively, proposed to be active and selective in propane oxidation to acrylic acid and ammoxidation to acrylonitrile.[12−16,20,25−29] In particular, the presence of the M1 phase in these catalysts is associated with their ability to activate propane selectively into acrylic acid and acrylonitrile.[16,18,20,28−31] The selectivity to acrylic acid over these model catalysts correlated with the extent of exposure of the surface *ab* planes of the M1 phase proposed to contain the active and selective surface sites.[18] A recent low energy ion scattering (LEIS) study of the M1 phases with the bulk Mo−V−Te−O compositions indicated that the surfaces of these catalysts are terminated with

* Address correspondence to this author. Phone: +1-513-556-0203. Fax: +1-513-556-3473. E-mail: vadim.guliants@uc.edu.

† Current address: ABB Lummus Global Inc., Technology Development Center, 1515 Broad Street, Bloomfield, NJ 07003.

10.1021/jp056720f CCC: $33.50
Published on Web 03/04/2006

a monolayer, which possessed a different elemental composition from that of the bulk.[32] The rates of propane consumption and formation of propylene and acrylic acid depended on the topmost surface V concentration, whereas no dependence of these reaction rates on either the surface Mo or Te concentrations was observed. These findings suggested that the bulk Mo−V−Te−O structure may function as a support for the unique active and selective surface monolayer in propane oxidation to acrylic acid.

In this study we further examined the catalytic behavior of the orthorhombic Mo−V−O and Mo−V−Te−Nb−O phases in the propane (amm)oxidation reactions as well as their surface active sites employing methanol and allyl alcohol as chemical probe molecules. These orthorhombic phases exhibited vastly different behavior in propane (amm)oxidation reactions and, therefore, represented highly promising catalytic systems for the study of the surface active sites. The LEIS study indicated that the topmost surfaces of these catalysts were somewhat depleted in VO_x. Moreover, direct evidence was obtained that the topmost surface VO_x sites were preferentially covered by chemisorbed allyloxy species, whereas methanol was a significantly less discriminating species. These findings suggested that several surface VO_x sites located at the entrances to the hexagonal and heptagonal channels in the orthorhombic Mo−V−Te−Nb−O structure may be responsible for the selective 8-electron transformation of propane to acrylic acid and acrylonitrile.

Experimental Section

Synthesis and Physicochemical Characterization. The mixed Mo−V−O catalyst was prepared hydrothermally using ammonium paramolybdate (Alfa Aesar, 81−83% as MoO_3) and vanadyl(IV) sulfate (Alfa Aesar, 99.9%) as the metal oxide sources according to a reported procedure.[31] In a typical synthesis, ammonium paramolybdate (Alfa Aesar), 11.5 g, was dissolved in 35 mL of deionized water while stirring at room temperature. Vanadyl sulfate (Alfa Aesar), 8.7 g in 25 mL of deionized water, was added dropwise to the Mo solution under stirring. The resultant dark brown gel was placed in a Teflon-lined stainless steel autoclave and heated for 20 h at 175 °C. The black solid was filtered and dried at 80 °C for 12 h. This mixed metal oxide precursor was calcined at 500 °C for 2 h under flowing N_2 (40−60 cm^3/min) in a tubular furnace. The temperature was ramped to 500 °C at 5 °C/min^{-1}.

The mixed Mo−V−Te−Nb−O catalyst possessing the synthesis $Mo_{1.00}V_{0.30}Te_{0.16}Nb_{0.12}$ composition was prepared hydrothermally with ammonium paramolybdate (Alfa Aesar, 81−83% as MoO_3), vanadyl(IV) sulfate (Alfa Aesar, 99.9%), TeO_2 (Alfa Aesar, 99.99%), and $Nb_2(C_2O_4)_5 \cdot nH_2O$ (CBMM, assayed 20.5% Nb_2O_5) as the metal oxide sources according to a reported procedure.[17] The synthesis gel was placed in a Teflon-lined stainless steel autoclave and heated for 48 h at 175 °C. The black solid was washed with deionized water, dried for 12 h at 80 °C, and calcined at 500 °C for 2 h under flowing N_2 (40−60 cm^3/min) in a tubular furnace.

Propane oxidation was conducted at 350−450 °C with use of a 48 mL/min feed of 6.3 vol % of propane, 9.4 vol % of oxygen, 47.3 vol % of water vapor, and the balance of He and 0.5−1.0 g of catalyst packed in a $^3/_8$ in. quartz tubular microreactor in a programmable oven. Allyl alcohol oxidation was carried out at 250−340 °C employing a feed of 6 vol % of allyl alcohol, 13 vol % of oxygen (47.3 vol % of H_2O), and the balance of He. Allyl alcohol and water were injected as liquids from a syringe pump into a mixture of flowing oxygen and He at 150 °C to enable their complete vaporization. An HP 5890II gas chromatograph equipped with an FID and TCD was employed for the reaction product analysis. Propane ammoxidation was conducted under similar conditions with a feed of 6 vol % of propane, 7 vol % of ammonia, 17 vol % of oxygen, and the balance of He. A Shimadzu GC14 gas chromatograph equipped with an FID and TCD was employed for the reaction product analysis. The carbon balances agreed within 5 mol %.

TABLE 1: Surfaces Analyzed by LEIS in Methanol (MeOH) and Allyl Alcohol (AllOH) Chemisorption−Desorption Studies

experiment	subsequent treatments/measurements
	a. Mo−V−Te−Nb−O catalyst
sputtering	as such measurement
	atomic oxygen
	sputtering (1 ML)
heating	in situ heating (400 °C)
MeOH	atomic oxygen
	chemisorption (110 °C, 20 min, 21.5 mbar)
	desorption at 400 °C (standard)
	desorption (overnight treatment)
	atomic oxygen 1
	atomic oxygen 2
AllOH	atomic oxygen
	chemisorption 1 (110 °C, 20 min, 10 mbar)
	chemisorption 2 (110 °C, 20 min, 15 mbar)
	chemisorption at 400 °C (standard)
	atomic oxygen
	b. Mo−V−O catalyst
MeOH	atomic oxygen
	chemisorption (110 °C, 20 min, 2.3 mbar)
	desorption at 400 °C (standard)
	molecular oxygen 1 (400 °C, 15 min, 2.2 > 0.6 mbar)
	molecular oxygen 2 (400 °C, 22 min, 2.5 > 1.1 mbar)
AllOH	atomic oxygen
	chemisorption (110 °C, 20 min, 15.8 mbar)
	desorption at 400 °C (standard)

The Mo−V−O and Mo−V−Te−Nb−O catalysts were characterized by powder X-ray diffraction (XRD) employing a Siemens D500 diffractometer (Cu Kα radiation). The ICP elemental composition was determined with a Leeman Labs ICP/Echelle Spectrometer, Model PS1000 ICP, equipped with a Hildebrand Grid nebulizer and Mo, V, Te, and Nb elemental standards (Alfa Aesar). The BET surface areas were determined from the N_2 adsorption isotherms ($0.05 < P/P_o < 0.3$) at −196 °C employing a Micromeritics TriStar 3000 porosimeter.

Outermost Surface Characterization by LEIS. The LEIS analysis of the Mo−V−O and Mo−V−Te−Nb−O catalysts after kinetic studies was performed employing a Calipso LEIS system equipped with a highly sensitive double toroïdal analyzer (3000× that of other LEIS analyzers). The unique feature of this LEIS system is that the damage inflicted upon the surface is negligible due to the low ion doses.[33] The analysis was performed with both $^4He^+$ and $^{20}Ne^+$ ions at 3 and 5 keV, respectively, as described previously[32] in order to quantify the contributions of the surface O, Mo, V, Te, and Nb ions. The following surfaces were analyzed (Table 1): (1) the original surfaces, (2) the surfaces after treatment with atomic oxygen for 10 min to remove carbonaceous deposits and environmental contaminants, (3) the surface of the Mo−V−Te−Nb−O catalyst after sputtering of ca. 1 atomic layer (ML) with 5 keV Ne^+ ions, (4) the surface of the Mo−V−Te−Nb−O catalyst at 400 °C, and (4) the surfaces of both catalysts during probe molecule (methanol and allyl alcohol) chemisorption and desoprtion experiments.

Sputtering and in Situ Heating of Mo−V−Nb−Te−O Catalyst. The Mo−V−Te−Nb−O catalyst was first analyzed

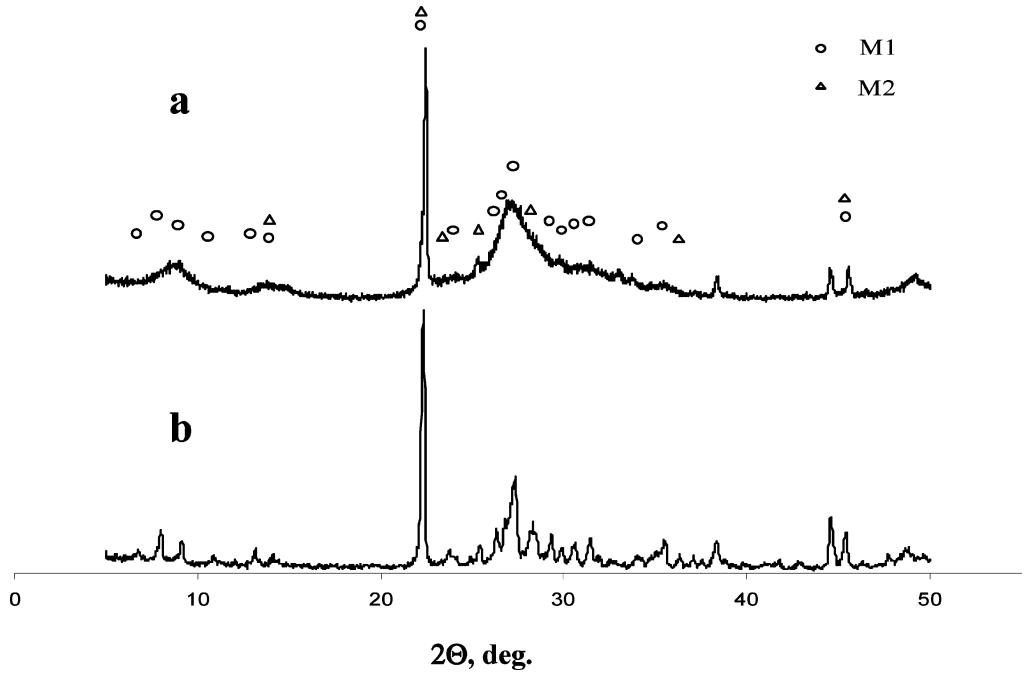

Figure 1. The XRD patterns: (a) the orthorhombic Mo−V−O phase and (b) Mo−V−Te−Nb−O catalyst. The peaks at ∼38.5 and 44.5° 2Θ are those of the Al sample holder.

as-received employing the 3 keV $^4He^+$ ions. The catalyst was then treated with atomic oxygen for 10 min to remove surface environmental contamination and analyzed with both 3 keV $^4He^+$ and 5 keV Ne^+ ions. A relatively small area of the catalyst tablet (1.8 × 1.8 mm^2) was then sputtered with 5 keV Ne^+ ions to remove approximately one monolayer from the surface. The sputtered area was measured with 3 keV $^4He^+$ and 5 keV Ne^+ ions. Subsequently, the catalyst tablet was heated in situ in a UHV analysis chamber of the LEIS instrument to 400 °C, which is a representative temperature for the propane (amm)oxidation reactions. A fresh, unsputtered location on this catalyst was analyzed with 3 keV $^4He^+$ and 5 keV Ne^+ ions at 400 °C.

Surface Probe Chemisorption and Desorption. The Mo−V−O and Mo−V−Te−Nb−O catalyst tablets were first treated with atomic oxygen for 10 min to remove environmental contamination and subsequently measured with 3 keV $^4He^+$ and, in the case of the Mo−V−Te−Nb−O catalyst, with both 3 keV $^4He^+$ and 5 keV Ne^+ ions.

The catalyst tablets were then transferred to a pretreatment chamber of the LEIS instrument where they were mounted onto a heating block. The tablets were heated to 110 °C prior to methanol (MeOH) and allyl alcohol (AllOH) chemisorption to minimize the occurrence of physisorption of these species at lower temperatures. The catalysts were then exposed to different alcohol vapor pressures depending on the temperature of liquid MeOH and AllOH sources. After the chemisorption step, the catalyst surfaces were measured with $^4He^+$ and Ne^+ ions. The probe molecule desorption was conducted by heating the catalysts at 10 deg/min to 400 °C. The catalysts were transferred to the UHV chamber for LEIS measurements after holding at 400 °C for 30 min. Subsequently, the Mo−V−Nb−Te−O catalyst was treated with atomic oxygen to remove the residual chemisorbed species and analyzed with $^4He^+$ and Ne^+ to establish whether the original clean surface was regenerated.

The Mo−V−O catalyst was treated with molecular oxygen at 400 °C at the end of the MeOH desorption step to investigate its ability to oxidize the residual chemisorbed species before the analysis with $^4He^+$ ions. This catalyst was heated at 10 deg/min to 400 °C and held at that temperature for 15 min. The oxygen pressure dropped from 2.2 mbar to 0.6 mbar when the catalyst was heated from room temperature to 310 °C and remained at 0.6−0.7 mbar during the remainder of the heating cycle. After the first treatment with molecular oxygen and subsequent $^4He^+$ measurement, the catalyst was treated with molecular oxygen for the second time and analyzed with $^4He^+$ ions.

Results

Synthesis, Composition, and Catalytic Behavior of Mo−V−O and Mo−V−Te−Nb−O Catalysts. The hydrothermal synthesis of the Mo−V−O and Mo−V−Te−Nb−O catalysts resulted in the formation of essentially pure orthorhombic (M1) phases (Figure 1). The XRD pattern of the Mo/V = 2 catalyst (Figure 1) corresponded to that of a less ordered M1 phase due to preferential crystallization of the M1 phase along the *c*-direction, which coincided with the long axis of the rodlike crystals of this Mo−V−O catalyst.[34] The *ab* planes of the M1 phase were oriented perpendicular to the long axis of the rodlike crystals, which was coincident with the *c*-direction in the M1 crystal.[34]

The elemental composition of the Mo−V−O catalyst was $Mo_{0.69}V_{0.31}O_x$ (by ICP analysis), which is close to its synthesis composition (i.e., Mo/V = 2) with a slightly lower V content. The bulk chemical composition of the Mo−V−Te−Nb−O catalyst ($Mo_{1.00}V_{0.27}Te_{0.17}Nb_{0.10}$) was also close to its synthesis composition ($Mo_{1.00}V_{0.30}Te_{0.16}Nb_{0.12}$). The Mo−V−O and Mo−V−Te−Nb−O catalysts possessed the BET surface areas of 6.6 and 7.0 m^2/g, respectively.

These two orthorhombic catalysts showed very different catalytic behavior in propane (amm)oxidation reactions (Table 2A,B). The Mo−V−Te−Nb−O catalyst was able to oxidize and ammoxidize propane much more actively and selectively than the Mo−V−O catalyst (Table 2A,B). Both catalysts performed better in propane ammoxidation than oxidation probably due to higher thermodynamic stability of acrylonitrile as compared to acrylic acid.[35] The Mo−V−O catalyst showed low selectivity to acrylic acid (∼4 mol %) and moderate

TABLE 2: Propane Oxidation over Mo−V−O and Mo−V−Te−Nb−O Catalysts at 380 °C, Propane Ammoxidation of over Mo−V−O and Mo−V−Te−Nb−O Catalysts at 380 °C, and Allyl Alcohol Oxidation over Mo−V−O and Mo−V−Te−Nb−O Catalysts

(A) Propane Oxidation over Mo−V−O and Mo−V−Te−Nb−O Catalysts at 380 °C[a]

catalyst	wt, g	flow rate, mL/min	$C(C_3H_8)$, mol %	$S(C_3H_6)$, mol %	S(AA), mol %	S(AceA), mol %	$S(CO_x)$, mol %	R
Mo−V−O	1.0	59	2	25	4	2	69	1.0
Mo−V−Te−Nb−O	0.5	21	49	1	58	10	29	16.4

(B) Propane ammoxidation of over Mo−V−O and Mo−V−Te−Nb−O catalysts at 380 °C[b]

catalyst	wt, g	flow rate, mL/min	$C(C_3H_8)$, mol %	$S(C_3H_6)$, mol %	S(ACN), mol %	S(AN), mol %	$S(CO_x)$, mol %	R
Mo−V−O	0.2	50	4	50	24	12	14	8.0
Mo−V−Te−Nb−O	0.2	12	58	3	79	9	9	26.4

(C) Allyl alcohol oxidation of over Mo−V−O and Mo−V−Te−Nb−O catalysts[c]

catalyst	wt, g	T, °C	flow rate, mL/min	C(AllOH), mol %	S(AA), mol %	S(Acr), mol %	$S(CO_x)$, mol %	R
Mo−V−O								
dry feed	0.03	250	29	15	3	83	14	2.6
wet feed	0.03	250	29	35	7	72	21	6.3
wet feed	0.03	300	39	67	6	53	41	16.4
Mo−V−Te−Nb−O								
dry feed	0.1	250	39	15	3	93	4	1.0
dry feed	0.1	300	19	84	21	66	13	2.9
wet feed	0.1	300	39	27	75	11	14	1.9

[a] Feed: 6.3 vol % of propane, 9.4 vol % of oxygen, 47.3 vol % of H_2O and the balance He. AA: acrylic acid; AceA: acetic acid; CO_x: carbon oxides. R = normalized rate of propane consumption. [b] Feed: 6 vol % of propane, 7 vol % of ammonia, 17 vol % of oxygen and the balance He. ACN: acrylonitrile; AN: acetonitrile; CO_x: carbon oxides. R = normalized rate of propane consumption. [c] Feed: 6 vol % of allyl alcohol, 13 vol % of oxygen (47.3 vol % of H_2O) and the balance He. AllOH: allyl alcohol; AA: acrylic acid; Acr: acrolein; CO_x: carbon oxides. R = normalized rate of allyl alcohol oxidation.

selectivity to propylene (up to 25 mol % at 380 °C) at low propane conversion (Table 2A,B) in agreement with previous observations.[31,34,36] The same catalyst displayed higher selectivity to propylene (50 mol %) and acrylonitrile (24 mol %) during propane ammoxidation. The presence of bulk Te and Nb oxide components in the M1 phase was highly beneficial for the selectivity of the Mo−V−Te−Nb−O catalyst to acrylic acid. This four-component M1 catalyst displayed 50 mol % selectivity to acrylic acid and 79 mol % selectivity to acrylonitrile. This catalyst further showed 44 mol % yield of acrylonitrile at 70% propane conversion at 380 °C.

Both catalysts were able to selectively oxidize allyl alcohol into acrolein in the absence of water vapor (Table 2C), while the rate of allyl alcohol oxidation over the Mo−V−O catalyst was nearly three times that over the Mo−V−Te−Nb−O catalyst (950 vs 360 nanomol/(s·m^2) at 15 mol % allyl alcohol conversion and 250 °C). However, both catalysts exhibited vastly different behavior during allyl alcohol oxidation in the presence of water vapor. Remarkably, the rate of allyl alcohol oxidation over the Mo−V−O catalyst increased more than 2-fold from 950 to 2270 nanomol/(s·m^2) at 250 °C, while it decreased over the Mo−V−Te−Nb−O catalyst from 1040 to 690 nanomol/(s·m^2) at 300 °C. More importantly, the Mo−V−Te−Nb−O catalyst displayed high selectivity to acrylic acid in the presence of water vapor (75 mol %), while the Mo−V−O catalyst still produced acrolein and increasing amounts of carbon oxides as the major reaction products. These observations strongly suggested that the Mo−V−Te−Nb−O catalysts contain the surface active sites capable of very selective oxidation of the acrolein intermediate to acrylic acid in the presence of water vapor.

Outermost Surface, Subsurface, and Bulk Composition of the Mo−V−Te−Nb−O Catalyst. Figure 2 shows the LEIS spectra measured for the atomic oxygen-treated Mo−V−Te−Nb−O catalyst prior to and after sputtering off one monolayer (1 ML). When compared with the bulk composition (Table 4, line 1), we found surface depletion for V (−23%) and Mo (−27%) and enrichment for Nb (+55%) and, particularly, Te (+165%) (Table 4, line 3). After sputtering off one monolayer (Table 4, line 4), the subsurface was depleted in V (−48%), whereas the Mo and Te concentrations came close to those observed in their bulk (−3% and −6%, respectively). The Nb enrichment increased to +170% when compared to the bulk composition of this catalyst.

Outermost Surface of the Mo−V−Te−Nb−O Catalyst at 400 °C. Figure 3 shows the LEIS spectra of the 4-component catalyst at room temperature and 400 °C. The LEIS data indicated that the composition of the outermost surface remained relatively unchanged after the catalyst was heated to 400 °C (Table 3, lines 2 and 4, and Table 4, lines 3 and 5), which is a typical temperature employed in propane oxidation and ammoxidation reactions.

Methanol Chemisorption−Desorption Study of the Mo−V−Te−Nb−O Catalyst. The Mo−V−Nb−Te−O catalyst was exposed to the increasing vapor pressures of MeOH (1−21.5 mbar) and the surface coverage with chemisorbed methoxy species was monitored with $^4He^+$ measurements. The results obtained showed that saturated monolayer coverage of chemisorbed methoxy species was obtained after ∼15 min of exposure to ∼5 mbar of MeOH at 110 °C (Table 3, line 6, and Table 4, line 7). Upon methanol chemisorption, we found a significant (40−65%) decrease of the LEIS signal for *all* surface metal oxide ions (Figure 4 and Table 4, line 7). The remaining "accessible" surface was relatively Mo/V-depleted and Nb/Te-enriched as compared to the original surface after atomic oxygen treatment (Figure 5 and Table 5, lines 1 and 2). Thus, the methanol species was preferentially chemisorbed at the surface VO_x and MoO_x sites.

Methanol desorption experiments were performed by heating the catalysts to 400 °C at 10 deg/min and maintaining this

TABLE 3: LEIS Signals Measured for the Mo−V−Te−Nb−O and Mo−V−O Catalysts (counts/nC × eV)

	samples/treatment		3 keV $^4He^+$ O	3 keV $^4He^+$ V	3 keV $^4He^+$ (Mo + Te + Nb)	5 keV Ne^+ Mo	5 keV Ne^+ Nb	5 keV Ne^+ Te
	Mo−V−Te−Nb−O catalyst							
1	sputtering	as such measurement	479	83	1022			
2		atomic oxygen	864	182	1287	5037	724	2861
3		sputtering (1 ML)	832	150	1432	7563	1375	1365
4	heating	in-situ heating	858	174	1097	4435	747	2453
5	MeOH	atomic oxygen	864	182	1287	5037	724	2861
6		chemisorption	379	68	623	2212	388	1608
7		desorption	541	45	805	3096	575	2073
8		desorption overnight	477	103	717	2806	454	992
9		atomic oxygen 1	770	86	1144			
10		atomic oxygen 2	792	78	1188	5646	893	2426
11	AllOH	atomic oxygen	864	182	1287	5037	724	2861
12		chemisorption 1	339	42	676			
13		chemisorption 2	297	48	629	3820	689	2261
14		desorption	635	49	1233	4568	522	443
15		atomic oxygen	789	128	1364	6654	1209	926
	Mo−V−O catalyst							
16	MeOH	atomic oxygen	923	275	1433			
17		chemisorption	169	29	229			
18		desorption	506	95	865			
19		molecular oxygen 1	590	138	1012			
20		molecular oxygen 2	604	143	990			
21	AllOH	atomic oxygen	923	275	1433			
22		chemisorption	266	39	502			
23		desorption	662	154	1023			

TABLE 4: Elemental Surface Fractions in the Mo−V−Te−Nb−O and Mo−V−O Catalysts

	samples/treatment		surface fractions (atom %) VOx	MoOx	NbOx	TeOx	sum	relative surface fractions (sum = 100%) VOx	MoOx	NbOx	TeOx
	Mo−V−Te−Nb−O catalyst										
1	bulk composition (ICP0							13.6	69.6	5.6	11.2
2	sputtering	as such	4.8								
3		atomic oxygen	10.6	51.6	8.8	30.0	100.8	10.5	51.1	8.7	29.7
4		sputtering (1 ML)	7.5	70.3	15.9	10.9	104.5	7.1	67.2	15.2	10.5
5	heating	in situ heating	10.1	45.4	9.0	25.7	90.2	11.2	50.3	10.0	28.5
6	MeOH	atomic oxygen	10.6	51.6	8.8	30.0	100.8	10.5	51.1	8.7	29.7
7		chemisorption	3.9	22.6	4.7	16.8	48.1	8.2	47.1	9.8	35.0
8		desorption	2.6	31.7	7.0	21.7	62.9	4.1	50.4	11.1	34.5
9		desorption overnight	5.9	28.7	5.5	10.4	50.5	11.8	56.8	10.9	20.6
10		atomic oxygen 1	5.0								
11		atomic oxygen 2	4.5	57.8	10.8	25.4	98.5	4.6	58.7	11.0	25.8
12	AllOH	atomic oxygen	10.6	51.6	8.8	30.0	100.8	10.5	51.1	8.7	29.7
13		chemisorption 1	2.4								
14		chemisorption 2	2.8	39.1	8.3	23.7	73.9	3.8	52.9	11.3	32.0
15		desorption	2.8	46.8	6.3	4.6	60.5	4.7	77.2	10.4	7.7
16		atomic oxygen	7.4	68.1	14.6	9.7	99.8	7.4	68.2	14.7	9.7
	Mo−V−O catalyst										
17	bulk composition (ICP)							24.7	75.3		
18	MeOH	atomic oxygen	15.9	81.3			97.3	16.4	83.6		
19		chemisorption	1.7	13.0			14.7	11.4	88.6		
20		desorption	5.5	49.1			54.6	10.1	89.9		
21		molecular oxygen 1	8.0	57.5			65.5	12.2	87.8		
22		molecular oxygen 2	8.3	56.2			64.5	12.8	87.2		
23	AllOH	atomic oxygen	15.9	81.3			97.3	16.4	83.6		
24		chemisorption	2.3	28.5			30.8	7.3	92.7		
25		desorption	8.9	58.1			67.0	13.3	86.7		

temperature for 30 min. The results obtained (Figure 4 and Table 4, line 8) indicated that the chemisorbed methoxy species were only partially removed from the surface of the Mo−V−Te−Nb−O catalyst under such desorption conditions: ∼35% of the original surface remained covered with methoxy and other carbonaceous species. This catalyst was further heated at 400 °C for 2 h, kept overnight at 110 °C, and reheated again at 400 °C for 15 min. However, the LEIS results obtained indicated that the surface coverage by these carbonaceous species was essentially unaffected by this prolonged treatment as manifested in the combined elemental surface fractions in Table 4, line 9.

To investigate whether these residual surface carbonaceous species can be removed by oxidation, the Mo−V−Te−Nb−O catalyst was treated with atomic oxygen in two 5 min steps. The first 5 min treatment was sufficient to almost completely regenerate a clean surface as manifested in the LEIS surface oxygen signal (Table 3, line 9, and Table 4, line 10). However, the outermost surface composition after atomic oxygen treatment was different from that of the original clean surface (Figure 5 and Table 4, lines 3 and 11, and Table 5, lines 1 and 4). The surface became relatively V/Te-depleted and Mo/Nb-enriched.

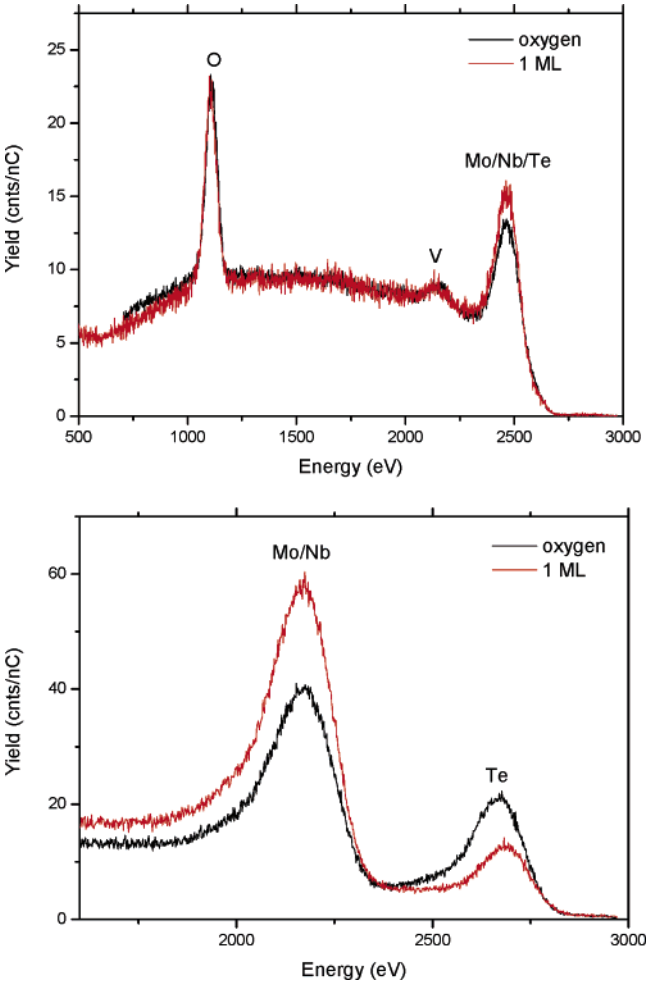

Figure 2. $^4He^+$ (top) and Ne^+ (bottom) spectra of the Mo−V−Te−Nb−O catalyst prior to and after sputtering off one monolayer (1 ML). Labels: oxygen = atomic-oxygen treated; 1 ML = after sputtering off 1 ML

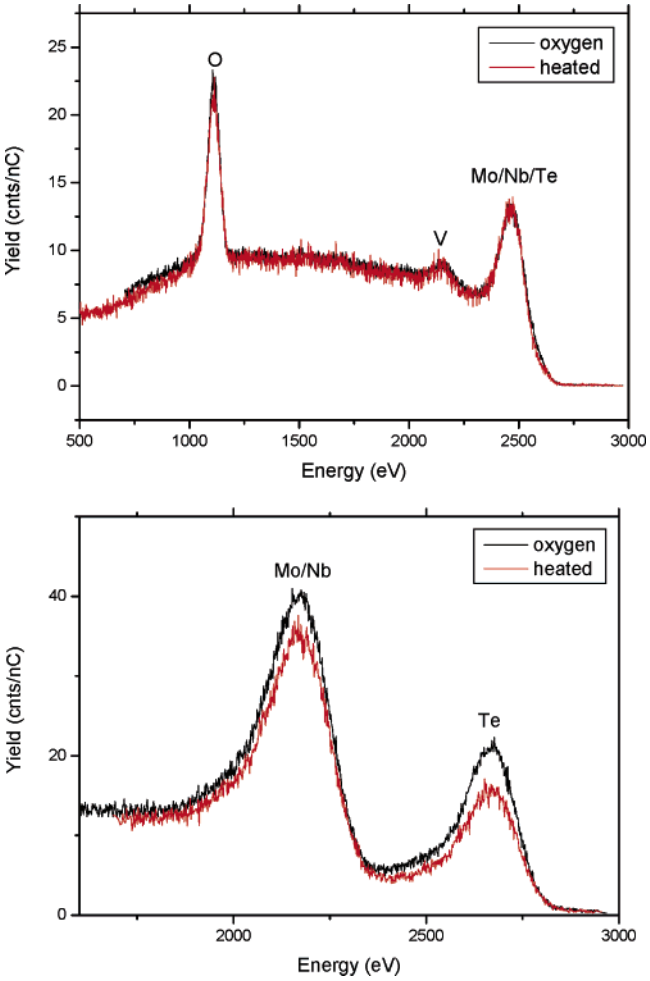

Figure 3. $^4He^+$ (top) and Ne^+ (bottom) spectra of the Mo−V−Te−Nb−O catalyst prior to and after in situ heating at 400 °C. Labels: oxygen = atomic-oxygen treated; heated = at 400 °C.

Allyl Alcohol Chemisorption and Desorption Study of the Mo−V−Te−Nb−O Catalyst. The allyl alcohol chemisorption study indicated that this species is selectively chemisorbed at the VO_x sites and significantly less at the surface Mo, Te, and Nb oxide sites in the following order: V ≫ Mo ∼ Te > Nb (Figures 6 and 7, Table 3, lines 11 and 13, Table 4, lines 12 and 14, and Table 5, lines 5 and 6). Similar to the findings of the MeOH chemisorption−desorption study, the attempted desorption of the surface allyloxy species at 400 °C under vacuum conditions resulted in significant V/Te-depletion and Mo/Nb-enrichment as compared to the original surface (Table 4, line 15, and Table 5, line 7). Nearly 40% of the surface was still covered with carbonaceous species at the end of the thermal desorption step (Tables 3, line 14, and Table 4, line 15). The surface V/Te depletion and Mo/Nb enrichment was also observed after the surface was regenerated by the atomic oxygen treatment (Figure 7).

Outermost Surface and Bulk Composition of the Mo−V−O Catalyst. The $^4He^+$ spectra of the Mo−V−O catalyst are shown in Figure 8. The elemental surface fractions (Table 4, line 18) indicated that the surface of this catalyst was V-depleted (−34%) and Mo-enriched (+11%) when compared with the bulk concentration (Table 4, line 17) in agreement with recent findings.[34]

Methanol Chemisorption−Desorption Study of the Mo−V−O Catalyst. The V and Mo signals have decreased to ∼11% and 16%, respectively, after methanol chemisorption (Table 5, line 10), whereas significantly greater surface area remained exposed in the case of the Mo−V−Te−Nb−O catalyst (V 37%; Mo 44%; Table 5, line 2). This indicated much higher methoxy coverage at the surface of the Mo−V−O catalyst. The elemental LEIS signals increased to 35% (V) and 60% (Mo) of the original clean surface after attempted desorption at 400 °C (Table 5, line 11). As in the case of the Mo−V−Te−Nb−O catalyst, the chemisorbed species were removed only partially and ∼45% of the original surface remained covered with surface methoxy and other carbonaceous species as seen in the combined elemental surface fractions reported in Table 4, line 20.

The Mo−V−O catalyst was treated after the desorption step with *molecular* rather than *atomic* oxygen. However, the accessible surface coverage increased only slightly, from 55% to 65%, after such treatment (Table 4, lines 20 and 21). A repeated molecular oxygen treatment was ineffective in removing additional surface species as seen from Figure 8 and the combined elemental surface fractions in Table 4, line 22. As compared to the original surface, the surface after molecular oxygen treatments became V-depleted and Mo-enriched manifested in relative VO_x and MoO_x surface fractions of 0.52 and 0.69 (Figure 9 and Table 5, lines 9 and 13).

Allyl Alcohol Chemisorption−Desorption Study of the Mo−V−O Catalyst. After the allyl alcohol chemisorption, the V and Mo signals decreased by 86% and 65%, respectively (Table 5, line 15). Similar to that observed for the Mo−V−Te−Nb−O catalyst, the allyl alcohol species appeared to be selectively absorbed at the VO_x sites (Figures 8 and 10, Table

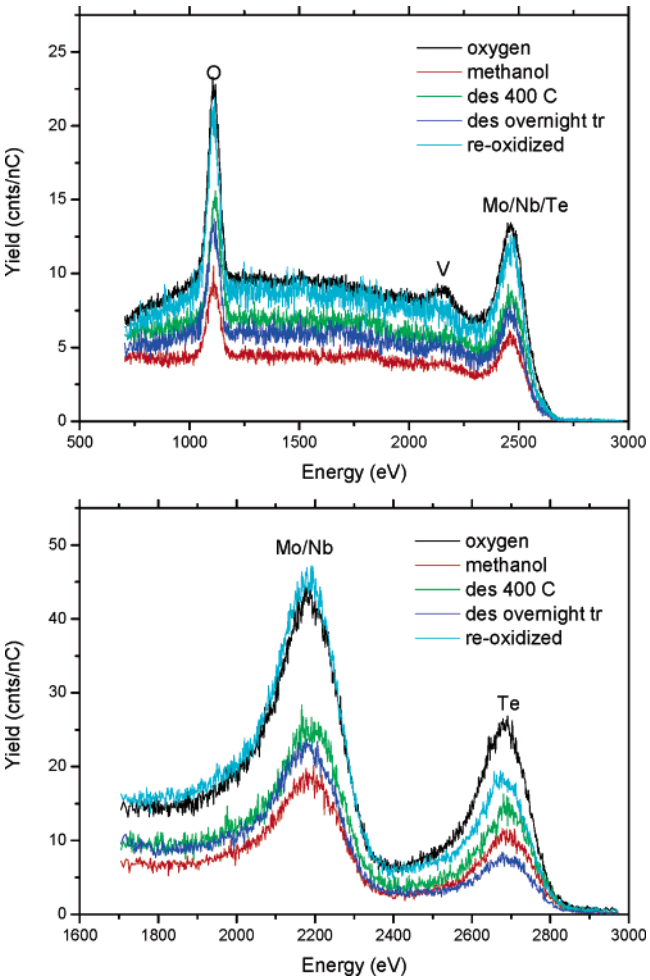

Figure 4. $^4He^+$ (top) and Ne^+ (bottom) spectra of the Mo−V−Te−Nb−O catalyst measured during MeOH chemisorption−desorption study. Labels: oxygen = atomic-oxygen treated; methanol = after methanol chemisorption; des 400 °C = after desorption at 400 °C; des overnight tr = after overnight desorption; re-oxidized = after atomic oxygen treatment.

4, line 24, and Table 5, line 15). Above 30% of the surface remained covered with allyl alcohol and other carbonaceous species after standard desorption at 400 °C (Table 3, line 23, and Table 4, line 25). However, the Mo−V−O catalyst tablet cracked during subsequent atomic oxygen treatment and the final LEIS measurements for this catalyst were not performed.

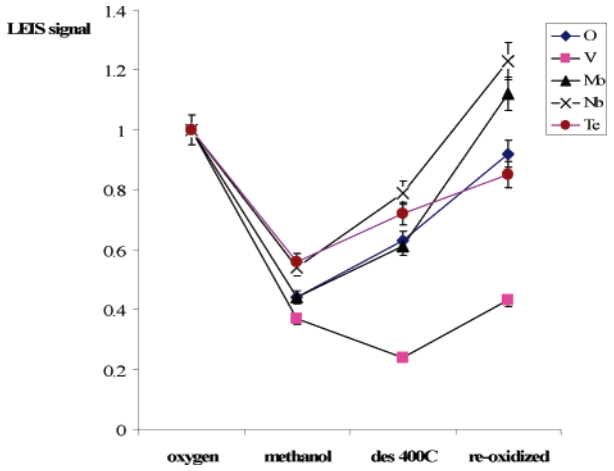

Figure 5. LEIS signals of the Mo−V−Te−Nb−O catalyst during MeOH chemisorption−desorption study normalized to those of the original atomic-oxygen treated Mo−V−Te−Nb−O surface. Labels: same as in Figure 4.

Discussion

The orthorhombic Mo−V−O and Mo−V−Te−Nb−O catalysts employed in the present study displayed vastly different behavior in the oxidation and ammoxidation of propane and oxidation of allyl alcohol. The Mo−V−Te−Nb−O catalyst was highly active and selective to both acrylic acid and acrylonitrile, whereas the Mo−V−O catalyst showed low selectivity in these two reactions. Moreover, the study of allyl alcohol oxidation over the Mo−V−O and Mo−V−Te−Nb−O catalysts demonstrated that the latter catalyst contained the surface active sites capable of very selective oxidation of the acrolein intermediate to acrylic acid in the presence of water vapor.

To understand the differences in catalytic behavior of these phases, we employed the chemisorption of methanol and allyl alcohol probe molecules to characterize the chemical nature of the surface active sites present in the orthorhombic Mo−V−O and Mo−V−Te−Nb−O catalysts. Methanol was employed as a probe to determine the number of surface active sites[37] of the orthorhombic Mo−V−O and Mo−V−Te−Nb−O catalysts of the present study, whereas allyl alcohol was further investigated as a new surface probe molecule due to its similarity to possible surface intermediates during propane (amm)oxidation.

Wachs et al.[38−40] demonstrated that methanol chemisorbs as a stable monolayer of surface methoxy species on an oxide

TABLE 5: Surface Compositions Relative to Compositions of Original Clean Surfaces

			relative surface compositions (atomic oxygen = 1.00)				
	samples/treatment		O	V	Mo	Nb	Te
	Mo−V−Te−Nb−O catalyst						
1	MeOH	atomic oxygen	1.00	1.00	1.00	1.00	1.00
2		chemisorption	0.44	0.37	0.44	0.54	0.56
3		desorption	0.63	0.24	0.61	0.79	0.72
4		atomic oxygen	0.92	0.43	1.12	1.23	0.85
5	AllOH	atomic oxygen	1.00	1.00	1.00	1.00	1.00
6		chemisorption	0.34	0.26	0.76	0.95	0.79
7		desorption	0.73	0.27	0.91	0.72	0.15
8		atomic oxygen	0.91	0.70	1.32	1.67	0.32
	Mo−V−O catalyst						
9	MeOH	atomic oxygen	1.00	1.00	1.00		
10		chemisorption	0.18	0.11	0.16		
11		desorption	0.55	0.35	0.60		
12		molecular oxygen 1	0.64	0.50	0.71		
13		molecular oxygen 2	0.65	0.52	0.69		
14	AllOH	atomic oxygen	1.00	1.00	1.00		
15		chemisorption	0.29	0.14	0.35		
16		desorption	0.72	0.56	0.71		

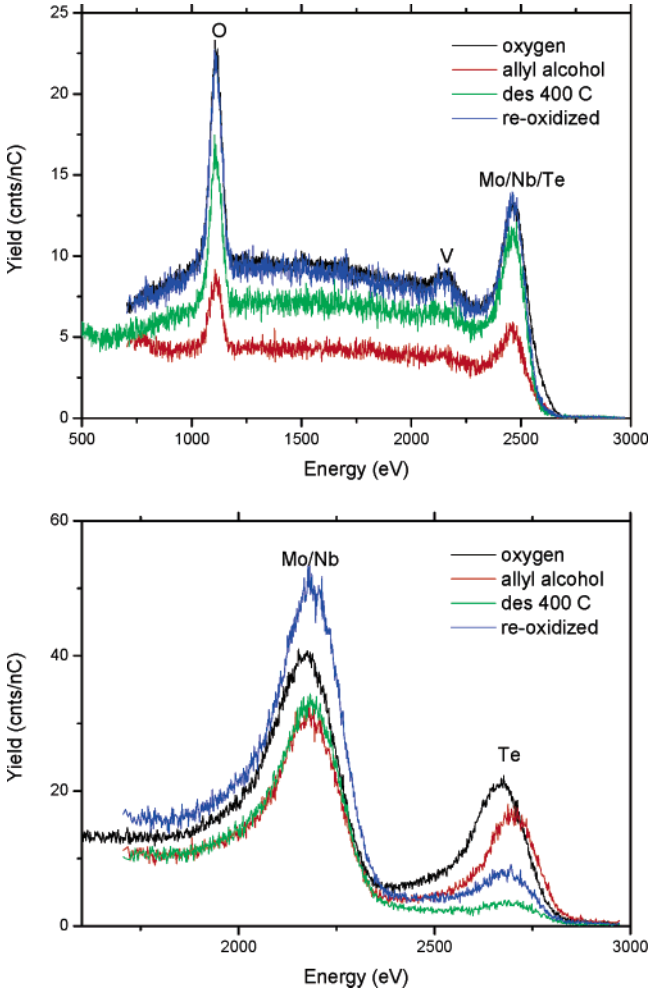

Figure 6. $^4He^+$ (top) and Ne^+ (bottom) spectra of the Mo−V−Te−Nb−O catalyst measured during AllOH chemisorption−desorption study. Labels: oxygen = atomic-oxygen treated; allyl alcohol = after allyl alcohol chemisorption; des 400 °C = after desorption at 400 °C; re-oxidized = after atomic oxygen treatment.

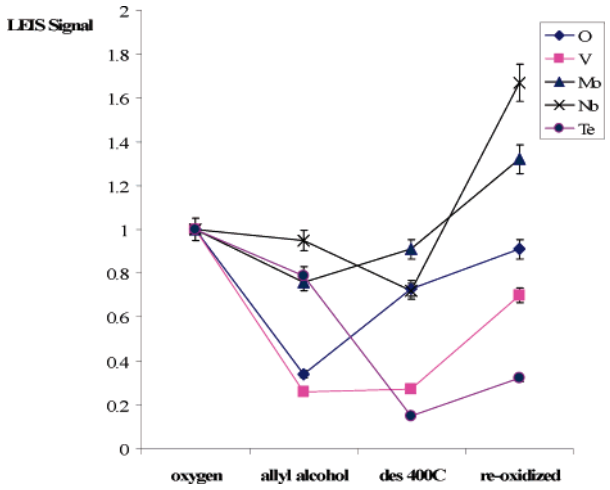

Figure 7. LEIS signals of the Mo−V−Te−Nb−O catalyst during AllOH chemisorption−desorption study normalized to those of original atomic-oxygen treated Mo−V−Te−Nb−O surface. Labels: same as in Figure 6.

surface exposed to an atmosphere of 2000 ppm of methanol in He at 100 °C. Surface methoxy species, $CH_3O_{(ads)}$, are also the reaction intermediates in the selective oxidation and dehydration of methanol and, therefore, the quantification of the amount of

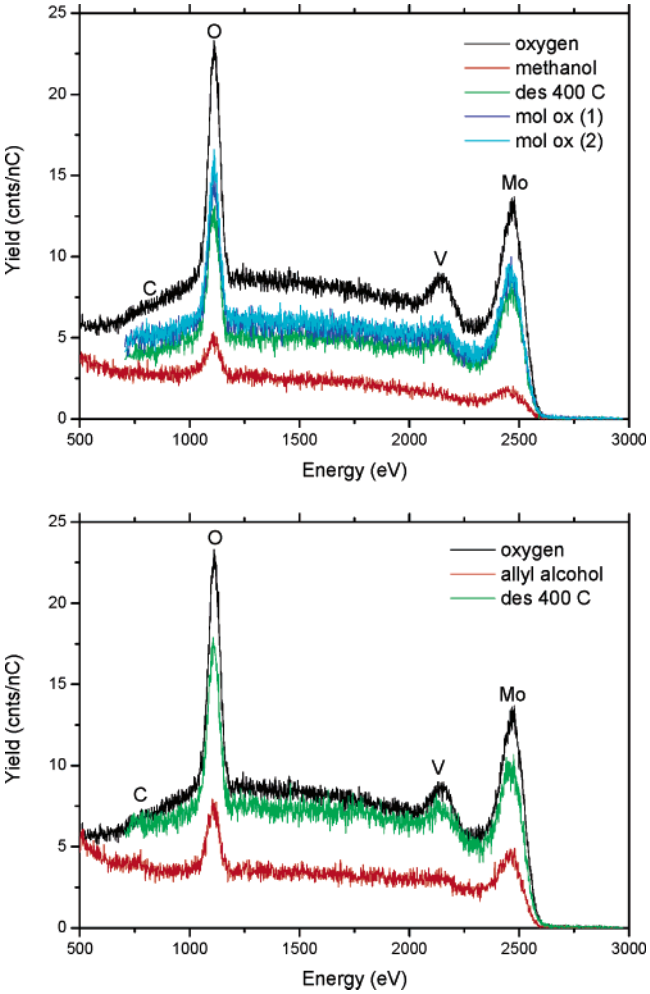

Figure 8. $^4He^+$ spectra of the Mo−V−O catalyst measured during MeOH (top) and AllOH (bottom) chemisorption−desorption studies. Labels: same as in Figures 4 and 6; mol ox (1) and (2) = molecular oxygen treatments 1 and 2.

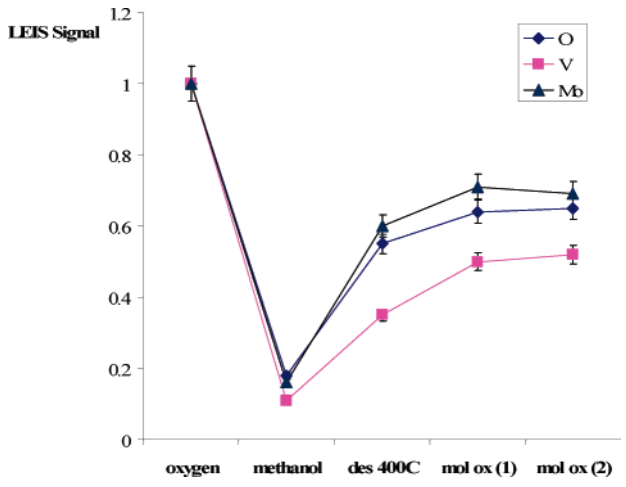

Figure 9. LEIS signals of the Mo−V−O catalyst during MeOH chemisorption−desorption study normalized to those of original atomic-oxygen treated Mo−V−O surface. Labels: same as in Figure 8.

surface methoxy species allows the quantitative determination of the density of surface active sites for methanol selective oxidation. Wachs et al.[41] recently applied methanol chemisorption followed by temperature programmed surface reaction (TPSR) to characterize the surfaces of orthorhombic $Mo_{0.6}V_{1.5}O_x$, $Mo_{1.0}V_{0.5}Te_{0.16}O_x$, and $Mo_{1.0}V_{0.3}Te_{0.16}Nb_{0.12}O_x$ catalysts. They

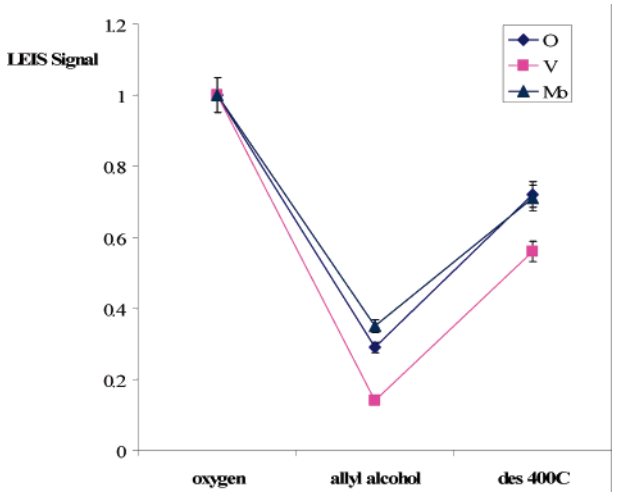

Figure 10. LEIS signals of the Mo−V−O catalyst during AllOH chemisorption−desorption study normalized to those of original atomic-oxygen treated Mo−V−O surface. Labels: same as in Figure 8.

observed that their Mo−V−O and Mo−V−Te−O catalysts yielded only formaldehyde from surface methoxy species on surface redox sites at ∼175 °C, which corresponded to V^{5+} sites promoted by adjacent cation ligands (i.e., Mo and Te). The $Mo_{1.0}V_{0.3}Te_{0.16}Nb_{0.12}O_x$ catalyst was found to yield both dimethyl ether formed at surface acidic Mo^{6+} sites and formaldehyde at the surface redox V^{5+} sites promoted by other surface cations, i.e., Te and Nb. Wachs et al. concluded from the analysis of methanol decomposition products that the surfaces of orthorhombic $Mo_{0.6}V_{1.5}O_x$, $Mo_{1.0}V_{0.5}Te_{0.16}O_x$, and $Mo_{1.0}V_{0.3}Te_{0.16}Nb_{0.12}O_x$ catalysts were enriched in V^{5+}, which they associated with the high mobility of the V^{5+} cations due to the low Tammann temperature of V_2O_5 as compared to other constituent bulk metal oxides in these mixed metal oxide catalysts.

The orthorhombic Mo−V−Te−Nb−O catalyst of our study was prepared by the same hydrothermal synthesis procedure and possessed a very similar bulk (ICP) elemental composition and catalytic performance as that employed by Wachs et al.[41] and Ueda et al.[31,36] The orthorhombic Mo−V−O catalyst of this study possessed a lower bulk Mo/V ratio than that used by Wachs et al.[41] and Ueda et al.[31,36] (2.2 vs 2.9). The LEIS study revealed that the topmost surface compositions in these two catalysts were different from their bulk compositions. Contrary to recent conclusions by Wachs et al. based on the indirect evidence of surface methoxy reactivity data, the LEIS data for of the Mo−V−Te−Nb−O catalyst (Tables 3 and 4) indicated surface depletion for V (−23%) and Mo (−27%), and enrichment for Nb (+55%) and, particularly, Te (+165%). The surface of the Mo−V−O catalyst was V-depleted (−34%) and Mo-enriched (+11%) as compared to its bulk composition in agreement with recent findings.[34] Only minor changes in the topmost surface composition were observed for the Mo−V−Te−Nb−O catalyst under the conditions of the LEIS experiments at 400 °C, which is a typical temperature employed in these propane transformation reactions. These findings strongly suggested that the bulk orthorhombic Mo−V−Te−Nb−O structure may function as a support for the unique active and selective surface layer in propane (amm)oxidation.

The Mo−V−O catalyst displayed higher surface coverage of chemisorbed alkoxy species than the Mo−V−Te−Nb−O catalyst (Tables 3 and 4). Nearly 50% of the Mo−V−Te−Nb−O and 85% of the Mo−V−O catalyst surface were covered with methoxy species after methanol chemisorption. The surface coverages of 27% and 68% were observed for these two catalysts during the allyl alcohol chemisorption experiments. When comparing the extent of participation of the surface MoO_x and VO_x sites in methanol chemisorption, we found only a slight preference for the VO_x sites (by a factor of ∼1.1) in both Mo−V−Te−Nb−O and Mo−V−O catalysts. Much greater difference was observed in the case of allyl alcohol chemisorption as the VO_x sites were 3.1 and 1.3 times more preferred than the MoO_x sites in the Mo−V−Te−Nb−O and Mo−V−O catalysts, respectively. The NbO_x and TeO_x sites showed the lowest activity in alcohol chemisorption (Figures 5 and 7 and Table 5) similar to recent observations by Wachs et al.[41]

Turning our attention to the results of the alcohol desorption experiments, we found that the chemisorbed species were removed from the surface only partially. We estimated that roughly 30% and 45% of the surface methoxy species desorbed from the surfaces of the Mo−V−Te−Nb−O and Mo−V−O catalysts, respectively, in the absence of atomic oxygen. It was further observed that the prolonged (overnight) desorption of the surface methoxy species from the Mo−V−Te−Nb−O catalyst was also ineffective (Table 4). Furthermore, this prolonged desorption resulted in a noticeable drop in combined elemental surface fractions. The subsequent atomic oxygen treatment to remove the residual carbonaceous species from the surface of the Mo−V−Te−Nb−O catalyst produced the surface in which the elemental fractions added up to ∼100%. However, this surface possessed a different elemental composition, namely a significant V/Te depletion and some Mo/Nb enrichment, indicative of a possible surface reconstruction induced by the conditions of the desorption experiment. No evidence of substantial surface reconstruction was found after methanol desorption from the surface of the Mo−V−O catalyst (Table 4 and Figure 9).

In the case of allyl alcohol, we similarly found that ∼50% of this species desorbed from the surface of the Mo−V−O catalyst. The surface of this catalyst after desorption did not exhibit an appreciable change in the surface Mo/V ratio (Table 4 and Figure 10). However, in the case of the Mo−V−Te−Nb−O catalyst the combined elemental surface fractions (Table 4) surprisingly decreased after the desorption experiment. While the surface VO_x fraction remained unchanged, the surface NbO_x and, in particular, TeO_x fractions decreased as the result of this treatment, while the surface MoO_x fraction increased. These results indicated that the surface allyloxy and other carbonaceous species changed their location or orientation at the surface. Moreover, the relative elemental surface fractions (Table 4) after desorption and atomic oxygen treatment were quite similar and, on the other hand, differed significantly from the elemental composition of the original surface (Figure 7). This suggested that the conditions of the desorption experiments resulted in a surface reconstruction of the Mo−V−Te−Nb−O catalyst with concomitant change in the location and orientation of surface allyloxy species. It was further observed that the surface reconstruction was much more pronounced after desorption of allyl alcohol than MeOH despite the fact that the surface coverage of this species was only half that of the methoxy species.

Therefore, this study indicated that allyl alcohol is a much more discriminating probe molecule than methanol to characterize the active surface sites present in the orthorhombic Mo−V−Te−Nb−O and Mo−V−O catalysts. However, the alcohol chemisorption and desorption experiments indicated that the single alcohol turnover investigated in this study was incomplete.

In principle, it is possible to determine the extent of participation of bulk and surface lattice oxygen via a Mars−van Krevelen reaction mechanism by performing several alcohol turnover cycles as was recently suggested by Wachs et al.[41] However, the ability to extract such mechanistic information was further complicated by irreversible surface reconstruction induced by the surface reactions of chemisorbed methanol and, in particular, allyl alcohol species observed in the present study.

Roles of Surface Metal Oxides in Propane Oxidation to Acrylic Acid. We further discussed our findings in light of recent hypothetical models of selective propane (amm)oxidation over the bulk Mo−V−Te−Nb−O catalysts based on the crystal structure of the orthorhombic Mo−V−Te−Nb−O phase.[29,30] According to the model proposed by Grasselli et al.,[30] the active and selective surface sites reside on the bulklike *ab* planes of the M1 phase and consist of an assembly of five metal oxide octahedra, $2V^{5+}/Mo^{6+}$, $1V^{4+}/Mo^{5+}$, $2Mo^{6+}/Mo^{5+}$, and two Te^{4+}−O sites, which are stabilized and structurally isolated from each other by four Nb^{5+} pentagonal bipyramidal centers. Te^{4+} cations predominantly occupy the hexagonal channels that run along the *c*-axis in the M1 structure. Nb is thought to play two important roles in the M1 structure: (1) by providing site isolation of the active centers from each other, which results in highly selective propane (amm)oxidation, and (2) stabilizing the crystal structure under catalytic reaction conditions. The propane-activating function of the M1 phase in this model is assigned to the V^{5+} sites of the catalytic center, while the two Te^{4+}−O sites are responsible for the α-H abstraction from the surface propylene intermediate. The resulting π-allyl intermediate is bonded to a neighboring Mo^{6+} of the active center, which is capable of either the NH or O insertion leading to acrylonitrile or acrylic acid (via acrolein), respectively.

In a model proposed by Ueda et al.,[36] the unique ability of the orthorhombic Mo−V−Te−Nb−O catalysts to activate propane selectively is associated with the presence of characteristic heptagonal channels in the M1 structure. In this model, propane is first activated on a Mo−O−V−O−H^+ site located in the surface of the heptagonal channel, which is followed by the allylic oxidation of propylene at the Mo(V)−O−Te−O site associated with the hexagonal channels and concluded by acrolein oxidation to acrylic acid over the former site, i.e., Mo−O−V−O−H^+. Acrylic acid is adsorbed at the surface TeO_x (and NbO_x) site, which retards its decomposition.

Our recent LEIS studies further pointed to the following catalytic functions of the constituent metal oxides in the orthorhombic Mo−V−M−O catalysts.[32,34] The Mo−V−O phase is capable of activating propane; however, it shows low catalytic activity and lacks the surface sites that are able to both bind the propylene intermediate strongly and oxidize it further to acrolein and acrylic acid. The addition of the M = Te, Sb, and Nb oxide species results in the formation of the surface V−O−M (and Mo−O−M) bonds and enhances the rates and selectivity of propane oxidation and formation of partial oxidation products. The surface TeO_x species are important for the allylic oxidation of the propylene intermediate, while the surface NbO_x in addition to the site isolation function moderates adsorption of reaction intermediates and products and prevents overoxidation of acrylic acid. The study of allyl alcohol oxidation over the Mo−V−O and Mo−V−Te−Nb−O catalysts further suggested that water plays a critical role during acrolein intermediate oxidation to acrylic acid over the Mo−V−Te−Nb−O M1 phase catalysts.

The present LEIS study of the orthorhombic Mo−V−O catalyst, which displayed poor selectivity during propane (amm)-oxidation reactions, indicated that the outermost surface of this catalyst was V-depleted with respect to its bulk composition. Although the surface structure of the orthorhombic Mo−V−O and Mo−V−Te−Nb−O phases is presently unknown, we attempted to interpret our findings in terms of the bulk structure of the *ab* planes of the orthorhombic Mo−V−Te−Nb−O phase recently reported by DeSanto et al.[29] The crystal structure of the orthorhombic Mo−V−O phase was suggested to have the same structural motif in which $4V^{5+}$ ions per unit cell occupy the Nb^{5+} pentagonal bipyramidal sites.[17,36] On the basis of the stoichiometry of the topmost surface of this phase determined by LEIS, it is expected that only the remaining 2 out of ∼6 V ions per surface unit cell in the *ab* plane would occupy crystallographically similar lattice sites along hexagonal and heptagonal channels they occupy in the crystal structure of the orthorhombic Mo−V−Te−Nb−O phase. By contrast, the LEIS analysis of the orthorhombic Mo−V−Te−Nb−O phase, which was much more selective in propane (amm)oxidation reactions, indicated that its topmost surface contained ∼6 V ions per unit cell area in the *ab* plane occupying the lattice sites along hexagonal and heptagonal channels. Although the V^{5+} pentagonal bipyramidal sites in the orthorhombic Mo−V−O phase may be capable of converting propane to propylene with modest selectivity (Table 2), such substitution of V^{5+} into the Nb^{5+} sites of the orthorhombic Mo−V−Te−Nb−O catalyst would disrupt the proposed active site isolation, which is expected to be detrimental for the selective (amm)oxidation of propane. Furthermore, on the basis of this structural analysis it appears that the selective 8-electron transformation of propane to acrylic acid and acrylonitrile may demand the presence of several surface VO_x redox sites lining the entrances to the hexagonal and heptagonal channels of the orthorhombic Mo−V−Te−Nb−O phase. It is interesting that these surface VO_x sites showed remarkable selectivity in allyl alcohol chemisorption relative to the surface MoO_x, TeO_x, and NbO_x sites, whereas the surface VO_x sites present on the Mo−V−O catalyst were significantly less discriminating. Higher coverage of methanol and allyl alcohol species observed at the surface of the Mo−V−O catalyst indicated that the surface TeO_x and NbO_x sites on the Mo−V−Te−Nb−O catalyst are unable to chemisorb these probe molecules to the same extent as the VO_x and MoO_x sites. This observation is further confirmed by the fact that the difference in the allyl alcohol surface coverage for the Mo−V−O and Mo−V−Te−Nb−O catalysts (∼41%) is very close to the sum of the surface TeO_x and NbO_x fractions in the Mo−V−Te−Nb−O catalyst (∼39%).

Moreover, the topmost surface of the orthorhombic Mo−V−Te−Nb−O catalyst showed a significant Te and slight Nb enrichment as compared to its bulk composition. For example, the bulk metal ion fractions in this catalyst were 65.0 (Mo), 17.4 (V), 11.0 (Te), and 6.7 atom % (Nb), whereas the topmost surface fractions of these metal ions (Table 4) corresponded to 51.1, 10.5, 29.7, and 8.7 atom %, respectively. The surface Te fraction (29.7 atom %) was significantly higher than the maximum Te content expected if all Te sites in the hexagonal and even heptagonal channels were fully occupied (16.7 atom % Te for the unit cell content of $M_{36}Nb_4Te_8$, M = Mo and V).[29] If we recall that only the topmost surface composition was found to be appreciably different from that of the bulk in the orthorhombic phases, it is apparent that at least half of the surface TeO_x species covered both surface MoO_x and VO_x sites. At present the catalytic roles of the surface V/Mo−O−Te (and V/Mo−O−Nb) sites created due to the surface TeO_x (and NbO_x) excess remain unclear.

Furthermore, if we assume that each of the 6 surface V^{5+} ions in the Mo−V−Te−Nb−O catalyst is a site for chemisorbed allyl alcohol, it would translate into ∼25% surface coverage based on the cross-sectional area of the allyl group (ca. 23.5 Å^2) and the unit cell area of the *ab* plane of the M1 phase (563.4 Å^2).[35] This estimate is very close to the experimentally observed allyl alcohol surface coverage for the Mo−V−Te−Nb−O catalyst (Table 4). Although at present we have no evidence that the topmost surfaces of the orthorhombic Mo−V−O and Mo−V−Te−Nb−O catalysts possess the structural motif of the bulk *ab* planes, the foregoing examination suggested that different surface locations for V^{5+} ions in the orthorhombic Mo−V−O and Mo−V−Te−Nb−O catalysts may be primarily responsible for vastly different catalytic behavior exhibited by these two orthorhombic phases. Finally, our findings strongly indicated that allyl alcohol is a highly promising probe molecule for the investigation of the surface active sites present in the bulk mixed metal oxide catalysts for selective (amm)oxidation of propane.

Conclusions

The present study demonstrated that chemical probe chemisorption combined with low energy ion scattering (LEIS) is a novel and highly promising surface characterization technique for the investigation of the active surface sites present in the bulk mixed metal oxides. The use of allyl alcohol as a discriminating chemical probe for the surface characterization of catalytic mixed metal oxides is particularly attractive because of the relevance of this molecule to products of propane (amm)-oxidation reactions. The specific goals of this study were to determine the outermost surface compositions and chemical nature of active surface sites present on the orthorhombic (M1) Mo−V−O and Mo−V−Te−Nb−O phases. While the Mo−V−Te−Nb−O phase was highly active and selective in propane oxidation to acrylic acid and ammoxidation to acrylonitrile, the Mo−V−O phase possessed low selectivity in these propane transformation reactions. Therefore, these orthorhombic phases represented highly promising catalytic systems for the study of the surface active sites.

The topmost surface of the Mo−V−Te−Nb−O catalyst was depleted in V and Mo and enriched in Nb and Te with respect to its bulk composition, while its subsurface and bulk compositions were similar. Only minor changes in the topmost surface composition were observed for this catalyst at 400 °C, which is a typical temperature employed in these propane transformation reactions. These findings strongly suggested that the bulk orthorhombic Mo−V−Te−Nb−O structure may function as a support for the unique active and selective surface monolayer in propane (amm)oxidation. Moreover, direct evidence was obtained that the topmost surface VO_x sites in the orthorhombic Mo−V−Te−Nb−O catalyst were preferentially covered by chemisorbed allyloxy species, whereas methanol was a significantly less discriminating probe molecule. The surface TeO_x and NbO_x sites on the Mo−V−Te−Nb−O catalyst were unable to chemisorb these probe molecules to the same extent as the VO_x and MoO_x sites. Our findings further suggested that different surface locations for V^{5+} ions in the orthorhombic Mo−V−O and Mo−V−Te−Nb−O catalysts may be primarily responsible for vastly different catalytic behavior exhibited by these two orthorhombic phases. Although the proposed isolated V^{5+} pentagonal bipyramidal sites in the orthorhombic Mo−V−O phase may be capable of converting propane to propylene with modest selectivity, the selective 8-electron transformation of propane to acrylic acid and acrylonitrile may demand the presence of several VO_x redox sites lining the hexagonal and heptagonal channels of the orthorhombic Mo−V−Te−Nb−O phase.

Acknowledgment. This research was supported by the Chemical Sciences, Geosciences and Biosciences Division, Office of Basic Energy Sciences, Office of Science, U.S. Department of Energy under Grant No. DE-FG02-04ER15604. The LEIS study was conducted with financial support of the National Science Foundation (international supplement to NSF CAREER CTS-0238962 to V.V.G.) and Rohm and Haas Co. The authors wish to thank Dr. R. S. Soman (University of Cincinnati) for the ICP elemental analysis and B. Swaminathan, L. Yuan, and L. Song for their help with catalytic studies of the Mo−V−O and Mo−Te−Nb−O catalysts.

References and Notes

(1) Thomas, J. M.; Thomas, W. J. *Principle and Practice of Heterogeneous Catalysis*; VCH Publications: New York, 1987.
(2) Satterfield, C. N. *Heterogeneous Catalysis in Practice*, 2nd ed.; McGraw-Hill: New York, 1991.
(3) Centi, G.; Cavani, F.; Trifirò, F. *Selective Oxidation by Heterogeneous Catalysis*; Kluwer Academic/Plenum Publishers: New York, 2001.
(4) Lin, M. *Appl. Catal. A* **2001**, *207*, 1.
(5) Grasselli, R. K. *Catal. Today* **1999**, *49*, 141.
(6) Bettahar, M. M.; Costentin, G.; Savary, L.; Lavalley, J. C. *Appl. Catal., A* **1996**, *145*, 1.
(7) Lin, M. *Appl. Catal., A* **2003**, **250**, 305.
(8) Lin, M. *Appl. Catal., A* **2003**, *250*, 287.
(9) Cavani, F.; Trifirò, F. *Catal. Today* **1999**, *51*, 561.
(10) Cavani, F.; Trifirò, F. *Stud. Surf. Sci. Catal.* **1997**, *110*, 19.
(11) Baerns, M.; Buyevskaya, O. *Catal. Today* **1998**, *45*, 13.
(12) Vitry, D.; Morikawa, Y.; Dubois, J. L.; Ueda, W. *Top. Catal.* **2003**, *23*, 47.
(13) DeSanto, P., Jr.; Buttrey, D. J.; Grasselli, R. K.; Lugmair, C. G.; Volpe, A. F.; Toby, B. H.; Vogt, T. *Top. Catal.* **2003**, *23*, 23.
(14) Grasselli, R. K.; Burrington, J. D.; Buttrey, D. J.; DeSanto, P., Jr.; Lugmair, C. G.; Volpe, A. F., Jr.; Weingand, T. *Top. Catal.* **2003**, *23*, 5.
(15) Holmberg, J.; Grasselli, R. K.; Andersson, A. *Top. Catal.* **2003**, *23*, 55.
(16) Baca, M.; Pigamo A.; Dubois, J. L.; Millet, J. M. M. *Top. Catal.* **2003**, *23*, 39.
(17) Vitry, D.; Morikawa, Y.; Dubois, J. L.; Ueda, W. *Appl. Catal., A* **2003**, *251*, 411.
(18) Guliants, V. V.; Bhandari, R.; Soman, R. S.; Guerrero-Perez, O.; Banares, M. A. *Appl. Catal., A* **2004**, *274*, 123.
(19) Lin, M.; Linsen, M. W. U.S. Patent 6,180,825, 2001, to Rohm and Haas Company (U.S.A.).
(20) Al-Saeedi, J. N.; Vasudevan, V. K.; Guliants, V. V. *Catal. Commun.* **2003**, *4*, 537.
(21) Ushikubo, T.; Koyasu, Y.; Nakamura, H.; Wajiki, S. JP 10045664, 1998, to Mitsubishi Chemical Corp.
(22) Ushikubo, T.; Oshima, K. JP 10036311, 1998, to Mitsubishi Chemical Corp. (JP).
(23) Hatano, M.; Kayou, A. European Patent 318,295 (1988), to Mitsubishi Chemical Corp. (JP).
(24) Ushikubo, T.; Oshima, K.; Kayo, A.; Umezawa, T.; Kiyona, K.; Sawaki, I. European Patent 529,853 (1992), to Mitsubishi Chemical Corp. (JP).
(25) Ushikubo, T.; Oshima, K.; Kayo, A.; Vaarkamp, M.; Hatano, M. *J. Catal.* **1997**, *169*, 394.
(26) Millet, J. M. M.; Roussel, H.; Pigamo, A.; Dubois, J. L.; Dumas, J. C. *Appl. Catal. A* **2002**, *232*, 77.
(27) Aouine, M.; Dubois, J. L.; Millet, J. M. M. *Chem. Commun.* **2001**, *13*, 1180.
(28) Botella, P.; Garcia-Gonzalez, E.; Dejoz, A.; Lopez Nieto, J. M.; Vazquez, M. I.; Gonzalez-Calbet, J. *J. Catal.* **2004**, *225*, 428.
(29) DeSanto, P., Jr.; Buttrey, D. J.; Grasselli, R. K.; Lugmair, C. G.; Volpe, A. F.; Toby, B. H.; Vogt, T.; Kristallogr, Z. **2004**, *219*, 152.
(30) Grasselli, R. K.; Buttrey, D. J.; DeSanto, P., Jr.; Burrington, J. D.; Lugmair, C. G.; Volpe, A. F., Jr.; Weingand, T. *Catal. Today* **2004**, *91*−*92*, 251.
(31) Katou, T.; Vitry, D.; Ueda, W. *Catal. Today* **2004**, *91*−*92*, 237.
(32) Guliants, V. V.; Bhandari, R.; Brongersma, H. H.; Knoester, A.; Gaffney, A. M.; Han, S. *J. Phys. Chem. B* **2005**, *109*, 10234.

(33) Maas, A. J. H.; Viitanen, M. M.; Brongersma, H. H. *Surf. Interface Anal.* **2000**, *30*, 3.
(34) Guliants, V. V.; Bhandari, R.; Swaminathan, B.; Vasudevan, V. K.; Brongersma, H. H.; Knoester, A.; Gaffney, A. M. *J. Phys. Chem. B* **2005**, *109*, 24046.
(35) *CRC Handbook of Chemistry and Physics*, 3rd electronic on-line edition based on 85th edition; CRC Press: Boca Raton, FL, 2004−2005; http://hbcpnetbase.com/.
(36) Ueda, W.; Vitry, D.; Katou, T. *Catal. Today* **2005**, *99*, 43.
(37) Tatibouet, J. M.; Lauron-Pernot, H. *J. Mol. Catal. A*: *Chem.* **2001**, *171*, 2005 and references therein.
(38) Briand, L. E.; Farneth, W.; Wachs, I. E. *Catal. Today* **2000**, *62*, 219.
(39) Burcham, L. J.; Briand, L. E.; Wachs, I. E. *Langmuir* **2001**, *17*, 6164.
(40) Briand, L. E.; Jehng, J.-M.; Cornaglia, L.; Hirt, A. M.; Wachs, I. E. *Catal. Today* **2003**, *78*, 257.
(41) Wachs, I. E.; Jehng, J.-M.; Ueda, W. *J. Phys. Chem. B* **2005**, *109*, 2275.